

Aerosol Inlet Characterization Experiment Report

RL Bullard C Kuang
J Uin S Smith
SR Springston

May 2017

DISCLAIMER

This report was prepared as an account of work sponsored by the U.S. Government. Neither the United States nor any agency thereof, nor any of their employees, makes any warranty, express or implied, or assumes any legal liability or responsibility for the accuracy, completeness, or usefulness of any information, apparatus, product, or process disclosed, or represents that its use would not infringe privately owned rights. Reference herein to any specific commercial product, process, or service by trade name, trademark, manufacturer, or otherwise, does not necessarily constitute or imply its endorsement, recommendation, or favoring by the U.S. Government or any agency thereof. The views and opinions of authors expressed herein do not necessarily state or reflect those of the U.S. Government or any agency thereof.

Aerosol Inlet Characterization Experiment Report

RL Bullard, Brookhaven National Laboratory (BNL)
Principal Investigator

C Kuang, BNL
J Uin BNL
S Smith, BNL
SR Springston, BNL
Co-Investigators

May 2017

Work supported by the U.S. Department of Energy,
Office of Science, Office of Biological and Environmental Research

Executive Summary

The U.S. Department of Energy (DOE) Atmospheric Radiation Measurement (ARM) Climate Research Facility Aerosol Observation System inlet stack was characterized for particle penetration efficiency from 10 nm to 20 μm in diameter using duplicate scanning mobility particle sizers (10 nm-450 nm), ultra-high-sensitivity aerosol spectrometers (60 nm- μm), and aerodynamic particle sizers (0.5 μm -20 μm). Results show good model-measurement agreement and unit transmission efficiency of aerosols from 10 nm to 4 μm in diameter. Large uncertainties in the measured transmission efficiency exist above 4 μm due to low ambient aerosol signal in that size range.

Acronyms and Abbreviations

AOS	Aerosol Observation System
APS	aerodynamic particle sizer
ARM	Atmospheric Radiation Measurement
C	Celsius
ccm	cubic centimeter
cm	centimeter
DOE	U.S. Department of Energy
ft	foot
GAW	Global Atmosphere Watch
ID	inside diameter
L	liter
m	meter
min	minute
nm	nanometer
NOAA	National Oceanic and Atmospheric Administration
SMPS	scanning mobility particle sizer
UHSAS	ultra-high-sensitivity aerosol spectrometer
μm	micrometer
WMO	World Meteorological Organization

Contents

Executive Summary	iii
Acronyms and Abbreviations	iv
1.0 Introduction	1
2.0 Experimental Approach.....	3
2.1 SMPS.....	3
2.2 UHSAS.....	4
2.3 APS	5
3.0 Results and Discussion.....	6
3.1 Model Results.....	6
3.2 Empirical Results	7
3.2.1 SMPS.....	7
3.2.2 UHSAS.....	8
3.2.3 APS	9
4.0 Conclusions and Future Work	11
5.0 References	11

Figures

1 AOS containers deployed in Manacapuru, Brazil during the Green Ocean Amazon campaign.	1
2 A) External view of AOS inlet stack. B) Flow distributor port with the center port oriented vertically and four outer ports 5 degrees from vertical (insulation removed for clarity).	2
3 Load of instruments on each flow distributor port on the AOS used for the Aerosol Inlet Characterization Experiment.	3
4 A) Line run to the top of the stack for the ambient measurement. B) Core inlet extractor from side flow distributor port. C) Coils used in SMPS experiment. D) Side-by-side SMPS measurements.	4
5 Fast-switching, three-way valve used for the UHSAS portion of inlet characterization.	5
6 Side-by-side APS sampling for instrument bias correction.	6
7 NOAA model for conditions during Aerosol Inlet Characterization Experiment.	6
8 SMPS inlet characterization details.	7
9 SMPS inlet characterization details for the scenario in which the SMPS sampling from ambient and the SMPS sampling from the stack are switched.	8
10 UHSAS inlet characterization details.	9
11 UHSAS inlet characterization details for single UHSAS experiment with 3-way valve.	9
12 APS inlet characterization details.	10
13 Composite inlet characterization with penetration efficiency results and NOAA model prediction.	11

1.0 Introduction

A proper characterization of size-dependent particle losses is essential when reporting ambient aerosol concentrations (Fuchs, 1964; Hinds, 1999; Belyaev, 1972). Instrument containers such as ARM's Aerosol Observation System (AOS) house and protect instruments while drawing air for ambient sampling (Baltensperger, 2003; Jefferson, 2011). The AOS inlet was designed to minimize particle losses over a wide range of aerosol sizes ($< 10 \mu\text{m}$) (Baltensperger, 2003; Liu, 1967; Ogren, 1995). This or equivalent observation systems have been used by ARM, the National Oceanic and Atmospheric Administration (NOAA), and the World Meteorological Organization (WMO)/Global Atmosphere Watch (GAW) for over 20 years (see Figure 1). Past characterizations of aerosol transport losses between the ambient and individual aerosol instruments have focused on models combining flow dynamics and aerosol sedimentation, diffusion, turbulent flow inertia, and both isoaxial and anisoaxial superisokinetic sampling effects (Weiden, 2009). The literature lacks empirical/experimental characterization of aerosol losses through AOS-like inlet systems.



Figure 1. AOS containers deployed in Manacapuru, Brazil during the Green Ocean Amazon 2014/15 campaign. Containers with similar stack dimensions and flows have been deployed elsewhere around the world.

The aerosol inlet is designed to sample at ~10 m above ground level. The various counting, sizing, aerosol optical, and aerosol composition instruments housed inside the AOS are exposed to the following major components of the interior flow path: 1) a rain guard and bug screen (optional), 2) 1000 L min^{-1} flow (turbulent) through 4.6 m of large-diameter (20 cm ID), powder-coated aluminum tubing (see Figure 2a), 3) a 2.1 m smaller-diameter tube (4.76 cm ID) that core-extracts a reduced 150 L min^{-1} flow (turbulent) from the center of the larger-diameter tubing, and 4) a flow distributor with five ports (see Figure 2b), each drawing 30 L min^{-1} through 25 cm of 1.59 cm (5/8") ID stainless-steel tubing. Downstream of the flow distributor port are the varied tube lengths required to distribute ambient aerosol to the instruments housed in the AOS. A bypass flow manifold provides the additional flow through each port so that total flow through each port is maintained at 30 L min^{-1} (see Figure 3). This study characterizes the size-dependent penetration of ambient aerosol from the entrance of the inlet stack to the exit of the flow distributor ports. Future work will include characterization of aerosol transmission downstream of the flow distributor.

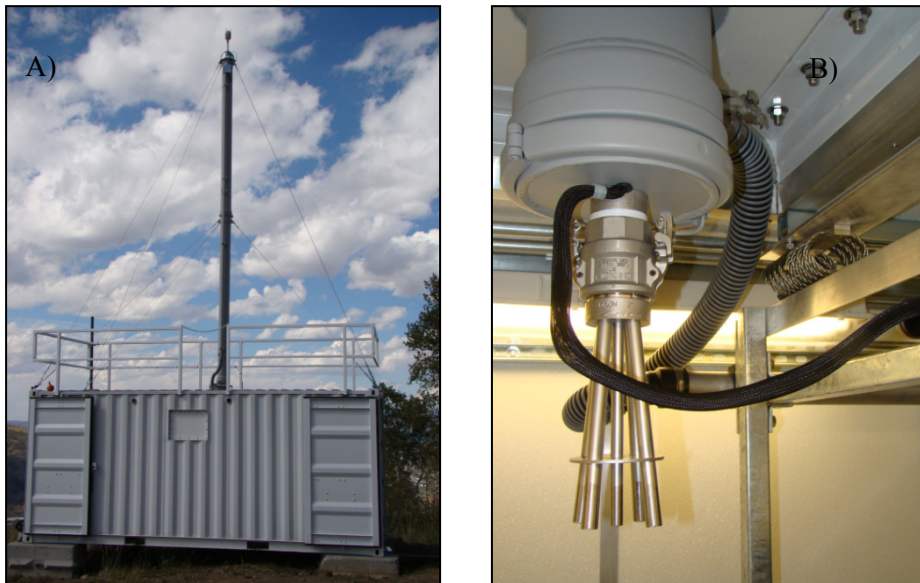


Figure 2. A) External view of AOS inlet stack with rain guard and bug screen and large-diameter, powder-coated aluminum tubing. B) Flow distributor port with the center port oriented vertically and four outer ports 5 degrees from vertical (insulation removed for clarity).

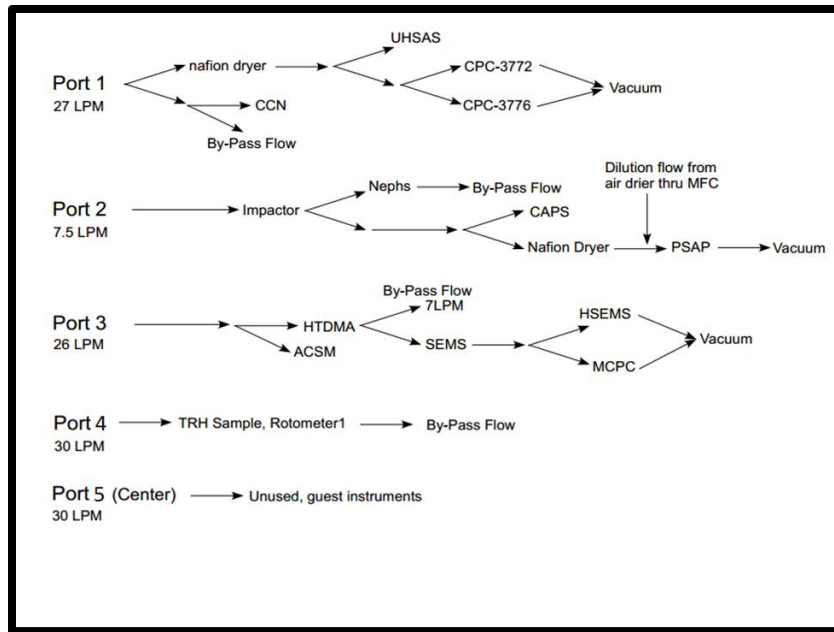


Figure 3. Load of instruments on each flow distributor port on the AOS used for the Aerosol Inlet Characterization Experiment.

2.0 Experimental Approach

Due to the physical dimensions and high sampling flow rate of the inlet stack, ambient atmospheric aerosol was used as the challenge aerosol for this characterization. The experimental approach is to measure the ambient aerosol size distribution at two locations: 1) sampling directly from the ambient (outside the container, near the stack inlet), and 2) sampling from the exit of the inlet flow distributor (inside the container). Any differences are due to the inlet (after accounting for instrument differences). Experiments involved simultaneous sampling from locations 1) and 2) to account for temporal variability in the aerosol size distribution and provide the long sample times needed to maximize counting signal. The instruments used in this characterization included two of each of the following: 1) (SMPS¹) scanning mobility particle sizer (Knutson, 1975) 2) (UHSAS²) an ultra-high-sensitivity aerosol spectrometer (Cai, 2008), and 3) (APS¹) aerodynamic particle sizer (Wilson, 1978). The SMPS sizes from 10 nm to 450 nm by charging and classifying aerosol based on electrical mobility. The UHSAS uses optical scattering and Mie theory to size aerosol from 60 nm to 1 μm . The APS sizes and counts aerosol from 0.5 μm to 20 μm by measuring the time of flight of aerosol accelerated through a nozzle.

2.1 SMPS

To directly sample aerosol from the ambient near the entrance of the inlet stack, one SMPS platform sampled through 50 ft. of $1/4$ " conductive tubing secured to the stack with a larger-diameter copper tube with 180° bend acting as a rain guard (see Figure 4a). To avoid additional bias from long tube lengths, the

¹ TSI Inc.; Shoreview, Minnesota.

² Droplet Measurement Technologies; Longmont, Colorado.

other SMPS platform sampled from a side (5° from vertical) flow distributor port, through a $5/8''$ to $1/4''$ stainless-steel core inlet extractor and an identical length (50 ft.) of “coiled” conductive tubing (see Figures 4b and 4c). The penetration efficiency is calculated by correcting the “raw” inlet characterization (stack SMPS platform versus ambient SMPS platform) for instrument-to-instrument bias and bias introduced by sampling through equivalent lengths of coiled versus straight tubing. Each of these tests (“raw” inlet characterization, instrument-to-instrument bias, and coil bias) took place over 1-2 days to accumulate sufficient counts in each size bin. A fourth test was conducted for verification, in which the SMPS sampling from ambient was switched with the SMPS sampling from the aerosol inlet stack.



Figure 4. A) Line run to the top of the stack for the ambient measurement, complete with rain guard. B) Core inlet extractor from side flow distributor port (used for SMPS and UHSAS). C) Coils used in SMPS experiment. D) Side-by-side SMPS measurements.

2.2 UHSAS

Due to long sample lines and the low inlet flow rate of the UHSAS (50 ccm), a TSI 3772 CPC (1 L min^{-1}) was used to provide extra transport flow to each UHSAS. The empirically measured corrections for coiled tubing and instrument intercomparison were also used to obtain the stack penetration efficiency. UHSAS instruments required additional tests with a single UHSAS and a three-way switching valve (see Figure 5). While this method removed the need for the instrument intercomparison correction, fast valve-

switching times were needed to avoid introducing additional errors due to temporal variation in the aerosol size distribution.



Figure 5. Fast-switching, three-way valve used for the UHSAS portion of inlet characterization.

2.3 APS

The low ambient coarse-mode aerosol concentrations made the inlet characterization in that size range more challenging, requiring much longer sampling times (~4 days) for each test. Because losses due to inertial impaction are more prevalent in the coarse mode, one APS (ambient) sampled ~4 m below the AOS inlet while the other APS (stack) sampled from the floor directly below the center flow distributor port to maintain sample lines equal in length and plumb to ensure no additional losses were introduced by tubing bends downstream of the flow distributor. In addition, the center flow distributor bypass connection was removed during these tests, changing the flow through the center distributor port from the nominal 30 L min^{-1} to the APS inlet flow rate (5 L min^{-1}). During long experiments, changes in the vertical mixing of the atmosphere could contribute to differences in the instrument comparison due to the 4 m separation between the ambient APS inlet and the AOS inlet. APS measurements also depend on a correction based on each instrument's avalanche photo-diode temperature. This characterization took place in February 2016 during a period of cold temperatures in which the AOS heating system was in use. Avalanche photo-diode temperatures varied by as much as $10 \text{ }^{\circ}\text{C}$ between the floor and the ceiling during tests. Instrument intercomparison samples were taken from the ambient through the center flow distributor and a stainless-steel "Y" fitting to both APS instruments (see Figure 6).



Figure 6. Side-by-side APS sampling for instrument bias correction.

3.0 Results and Discussion

3.1 Model Results

The modeled NOAA parameters were adjusted for the two sampling scenarios present in this study (see Figure 7). The SMPS and UHSAS sampled using 30 L min^{-1} from each flow distributor port with the instruments sampling from one of the four side ports at 5° degrees from vertical. The APS sampled directly from the center flow distributor port at 5 L min^{-1} without the additional 25 L min^{-1} of bypass flow.

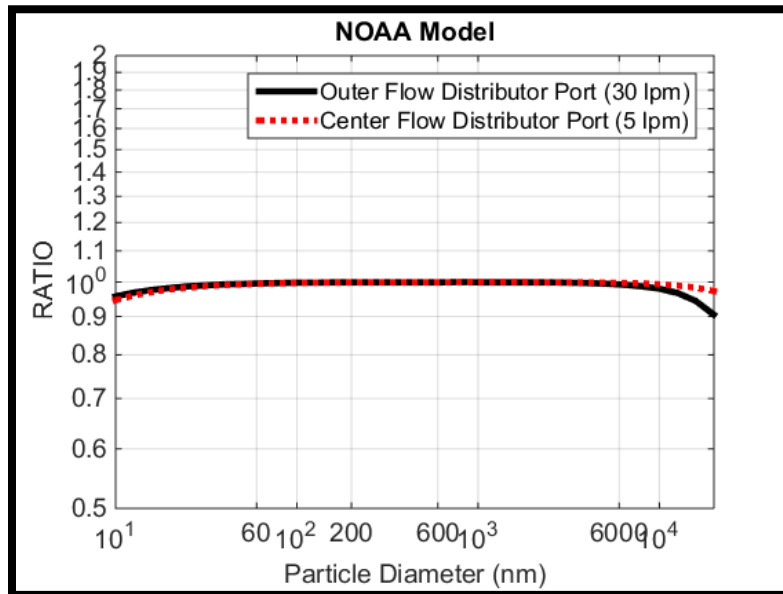


Figure 7. NOAA model for conditions during Aerosol Inlet Characterization Experiment.

3.2 Empirical Results

3.2.1 SMPS

The SMPS data were exported at eight size channels per decade, resulting in a total of 12 size bins covering the instrument detection range of 10 nm to 450 nm. Each sample accumulated counts over five minutes. The counts in each bin per five-minute scan was greater than 200 for all bins, making the error associated with random count statistics less than 10% in all sizes (often 1% or less). The ratio between the two SMPS platforms was calculated for each five-minute sample, creating an ensemble of ratios for each test (e.g., “raw” inlet characterization, instrument bias test, coil bias test). The size-dependent ratio and uncertainty for each test (see Figures 8 and 9) is reported as the average and standard deviation of the ensemble of ratios respectively. The final reported aerosol penetration efficiency with uncertainty is calculated by correcting the “raw” inlet characterization test ratio for instrument bias and coil bias ratios and propagating the associated uncertainties in these ratios. Figures 8 and 9 show the results from each test and the final measured penetration efficiency. Figures 8 and Figure 9 differ in which SMPS was sampling from the stack and which was sampling from ambient. Both scenarios show an agreement between model and measurement of 10% or less and within the uncertainty of the measurement.

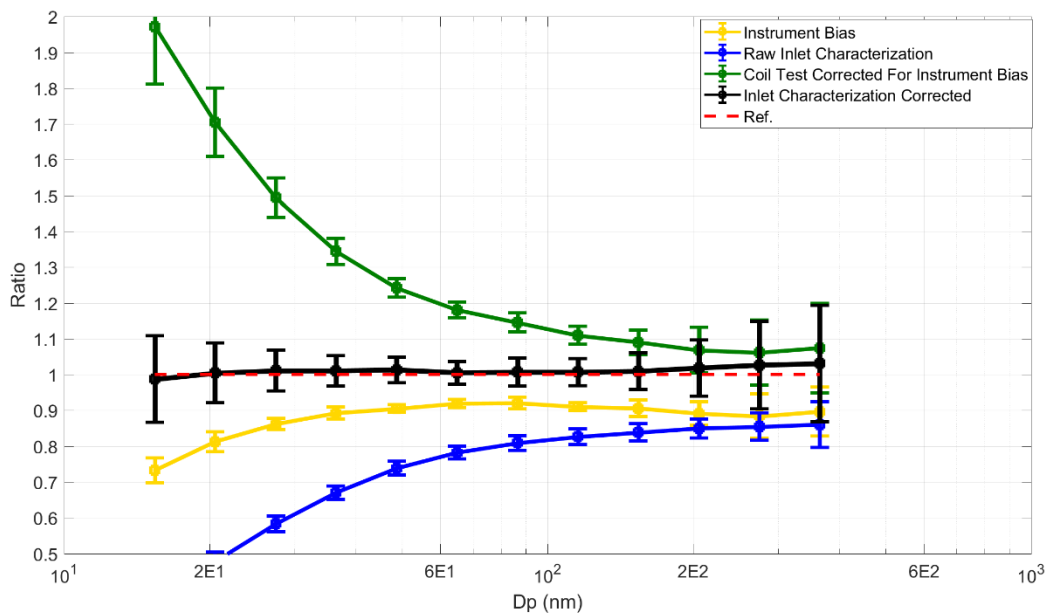


Figure 8. SMPS inlet characterization details.

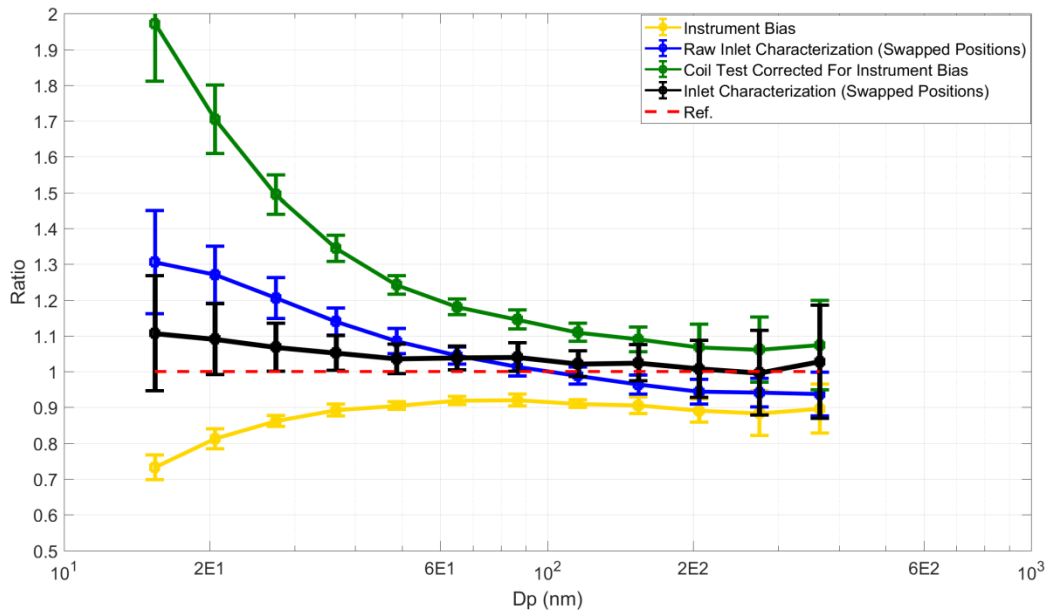


Figure 9. SMPS inlet characterization details for the scenario in which the SMPS sampling from ambient and the SMPS sampling from the stack are switched.

3.2.2 UHSAS

Like the SMPS, the UHSAS data were accumulated into broader particle diameter bins over a five-minute sampling interval. At times, individual bins contained 10 or less counts per sample, resulting in random count statistical relative errors that were as high as $\sim 30\%$. The same method for penetration efficiency calculation and uncertainty propagation used in the SMPS analysis was used for the UHSAS analysis. Figure 10 shows the results of each test and the final calculated penetration efficiency. Uncertainty is greatest in the largest particle diameters where signal was lowest. When a single UHSAS was used in conjunction with a three-way switching valve, the reported uncertainty was solely due to error in random count statistics. Quality assurance tests after the experiment showed a small leak in the three-way valve of less than 1 particle per cubic centimeter. Figure 11 shows the “raw” inlet characterization using a single UHSAS and a three-way valve, with the coil correction and the resulting stack penetration efficiency. The small leak in the three-way valve was not included in uncertainty calculations.

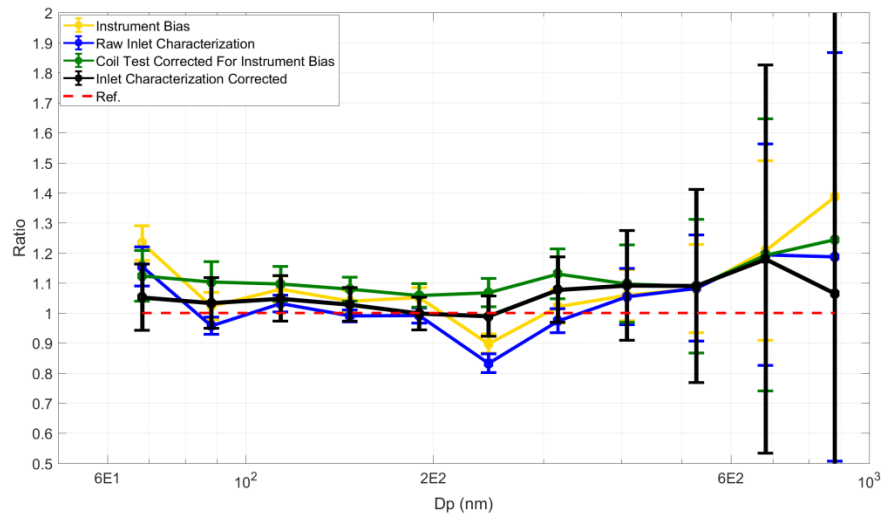


Figure 10. UHSAS inlet characterization details.

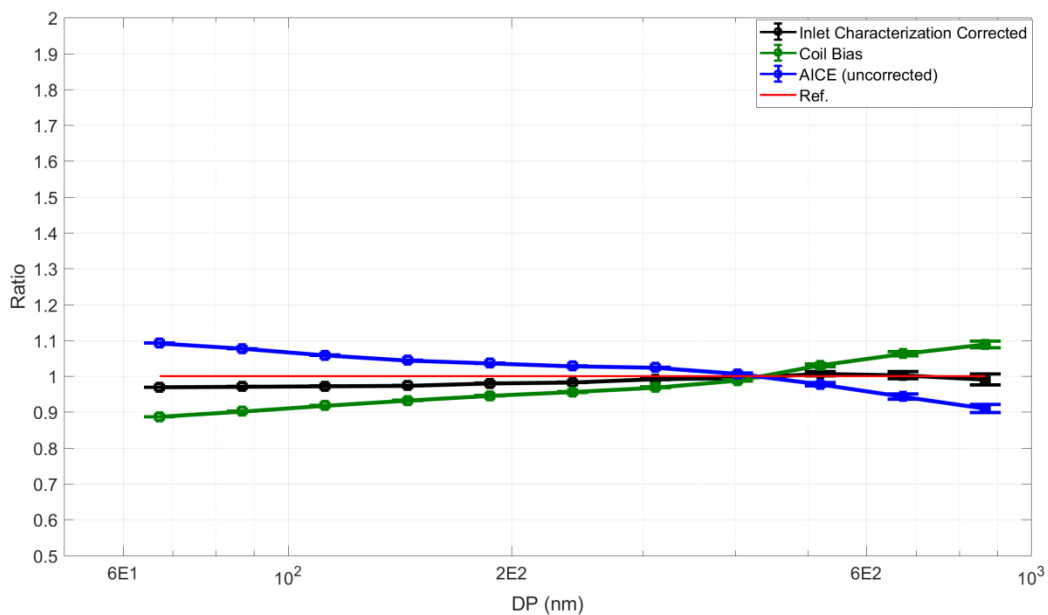


Figure 11. UHSAS inlet characterization details for single UHSAS experiment with 3-way valve.

3.2.3 APS

The APS data samples followed the same size binning resolution (8 size channels/decade) and time accumulation interval as the SMPS data samples. The accumulated counts were very low at the larger sizes ($> 5 \mu\text{m}$) with ~ 10 counts per five-minute sample and an error in counting statistics of $\sim 30\%$. The smaller sizes ($< 1 \mu\text{m}$) had additional systematic error introduced by the larger differences ($\sim 10^\circ\text{C}$) in the avalanche photo-diode temperatures between instruments, leading to changes in the instrument detection efficiency (at the smallest sizes) that were not accounted for in the instrument-to-instrument comparison. The same method used in the SMPS analysis for calculating an ensemble of ratios was implemented for

the APS analysis and showed a large degree of variability in the calculated ratios. The largest deviation from model predictions occurs at the lower and upper diameters (0.5 μm and 20 μm , respectively), and are likely attributable to avalanche photo-diode temperature differences and low counts, respectively. Figure 12 shows the results of all APS tests and the final calculated inlet efficiency in the coarse size range from 0.5 μm to 20 μm . The largest deviations from the NOAA model occur in the lower and upper size ranges.

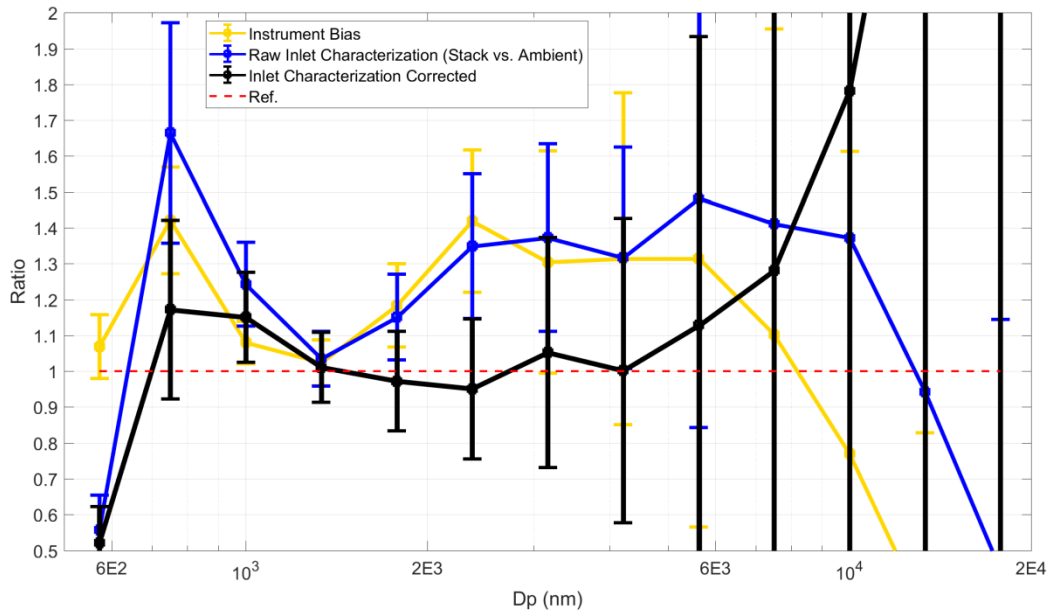


Figure 12. APS inlet characterization details.

Figure 13 shows the final penetration efficiency results with error bars and the NOAA-modeled prediction. The characterization spans the aerosol size distribution from 10 nm to 20 μm and shows a unit transmission efficiency from 10 nm to 20 μm , with large (> 50%) above 4 μm . The large uncertainties are likely attributable to counting statistics.

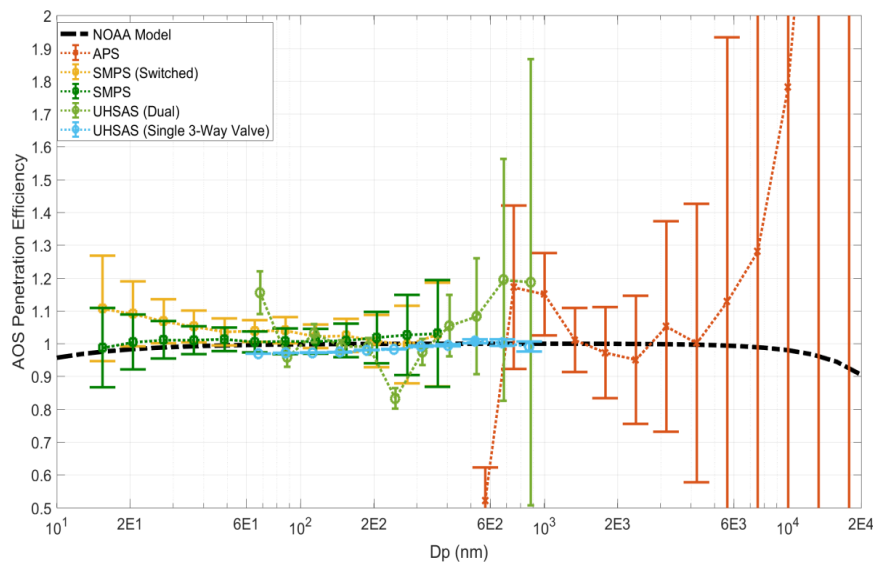


Figure 13. Composite inlet characterization with all penetration efficiency results and NOAA model prediction.

4.0 Conclusions and Future Work

The aerosol inlet characterization experiment measured the transmission efficiency through the AOS inlet (comprised of stack, inlet core extractor, flow distributor) spanning the aerosol size range from 10 nm up to 20 μm . Empirical results show unit transmission efficiency from 10 nm to 4 μm , in agreement with the NOAA model results within experimental uncertainty. Uncertainty is calculated based on variability in the ratio between samples over the course of each test and is propagated into calculated results.

Future work on inlet characterization will focus on longer sampling times for the APS portion of the characterization, which suffered from lack of signal in the larger size ranges (5 μm -20 μm) and errors associated with large differences in the avalanche photo-diode temperatures at the lower extreme (0.5 μm). The low counts merit a long-term measurement of \sim two weeks. These longer times should allow more time to accumulate good counting statistics. The experiment could make use of a three-way valve switching at five-minute intervals to connect the same APS to both the AOS stack inlet and a temporary inlet to ambient.

5.0 References

Baltensperger, U, L Barrie, C Fröhlich, J Gras, H Jäger, SG Jennings, SM Li, J Ogren, A Wiedensohler, C Wehrli, and J Wilson. 2003. WMO/GAW Aerosol measurement procedures, guidelines and recommendations. World Meteorological Organization Global Atmosphere Watch, [No. 153](#).

Belyaev, SP, and LM Levin. 1972. "Investigation of aerosol aspiration by photographing particle tracks under flash illumination." *Journal of Aerosol Science* 3(2):127-130, [doi:10.1016/0021-8502\(72\)90149-8](https://doi.org/10.1016/0021-8502(72)90149-8).

Cai, Y, DC Montague, WM-Bryan, and T Deshler. 2008. "Performance characteristics of the ultra high sensitivity aerosol spectrometer for particles between 55 and 800nm: Laboratory and field studies." *Journal of Aerosol Science* 39(9):759-769, [doi:10.1016/j.jaerosci.2008.04.007](https://doi.org/10.1016/j.jaerosci.2008.04.007).

Fuchs, NA. 1964. *The Mechanics of Aerosols*. Pergamon Press, London.

Hinds, WC. 1999. *Aerosol Technology: Properties, Behavior, and Measurement of Airborne Particles*. 2nd Edition, Wiley-John Wiley & Sons, New York.

Jefferson, A. 2011. Aerosol Observing System (AOS) Handbook. U.S. Department of Energy. [DOE/SC-ARM-TR-014](https://doi.org/10.2172/1013115).

Knutson, EO, and KT Whitby. 1975. "Aerosol classification by electric mobility: apparatus, theory, and applications." *Journal of Aerosol Science* 6(6):443-451, [doi:10.1016/0021-8502\(75\)90060-9](https://doi.org/10.1016/0021-8502(75)90060-9).

Liu, BYH, and DYH Pui. 1981. "Aerosol sampling inlets and inhalable particles." *Atmospheric Environment* 15(4): 589-600, [doi:10.1016/0004-6981\(81\)90190-6](https://doi.org/10.1016/0004-6981(81)90190-6).

Ogren, JA. 1995. A systematic approach to in situ observations of aerosol properties. In *Aerosol Forcing of Climate*, ed. RJ Charlson and J Heintzenberg, John Wiley & Sons, New York, pp. 215-226.

Von der Weiden, S-L, F Drewnick, and S Borrmann. 2009. "Particle loss calculator—a new software tool for the assessment of the performance of aerosol inlet systems." *Atmospheric Measurement Techniques* 2(2):479-494, [doi:10.5194/amt-2-479-2009](https://doi.org/10.5194/amt-2-479-2009).

Wilson, JC, and BYH Liu. 1980. "Aerodynamic particle size measurement by laser-doppler velocimetry." *Journal of Aerosol Science* 11(2):139-150, [doi:10.1016/0021-8502\(80\)90030-0](https://doi.org/10.1016/0021-8502(80)90030-0).

